Ann. Telecommun. (2013) 68:219–230
DOI 10.1007/s12243-012-0335-6

A robust invariant bipolar representation for R^3 surfaces: applied to the face description

Faouzi Ghorbel · Majdi Jribi

Received: 27 January 2012 / Accepted: 25 September 2012 / Published online: 19 October 2012

Abstract In this paper, we intend to introduce a novel invariant curved surface representation under the 3D motion group. It is constructed from the superposition of the two geodesic potentials generated from a given couple of surface points. By sampling this continuous representation, invariant points are extracted from a large neighborhood around these reference points. Different numerical methods are implemented in order to find an efficient approximation in the mean of the shape distance. The inference of small distortions of points positions applied to the reference points is analyzed. We apply the proposed representation to real 3D images. The experimentations are performed on the 3D facial database Bosphorus.

Keywords Bipolar surface representation · Geodesic potential · Invariant · 3D mesh · Hausdorff distance · Face analysis · Robustness · Shape space

1 Introduction

Actually, it is recognized that the description and the understanding of the 3D shapes play an important role in pattern recognition, computer vision, computer graphics coding, 3D compression, and 3D movement analysis. Thus, one of the major challenges faced today in the three-dimensional imaging field is the construction of a surface representation that ensures several properties such as the independence from the point of view, the robustness with respect to small local variations in shapes, the invariance under different parameterizations, and the accuracy that can be verified by the absolute completeness or at least by a kind of a local completeness.

In practice, the description of R^3 surfaces remains an open question in the sense of the four criteria described above and because of the fact that the data obtained from the 3D digital sensors are not organized or at least partially organized like the representation with a 3D triangular mesh. To highlight this issue, several past works have been performed in the area of accurate 3D shape descriptions. The three-dimensional surface description methods can be classified into four major categories: the transform-based approaches, the 2D views, the graph ones, and those based on statistical features.

The transform-based approaches consist in the application of specific transformations on the surface after its conversion onto 3D voxels or a spherical grid. The most known transformations are 3D Fourier [1, 2], the 3D Radon [3], the spherical trace transform [4], the angular radial transform [5], the radicalized extent function [6], the rotation-invariant spherical harmonics [7], the uniformization [8, 9], the concrete radicalized spherical projection [10], and the spherical wavelet descriptors [11].

For the two-dimensional view-based methods, a collection of 2D projections from canonical viewpoints is realized. Then, planar image descriptors are computed as Zernike moments [12] and Fourier descriptors [13].

F. Ghorbel · M. Jribi (✉)
GRIFT Research Group, CRISTAL Laboratory,
Ecole Nationale des Sciences de l'Informatique (ENSI),
La Manouba University, 2010 La Manouba, Tunisia
e-mail: majdi.jribi@ensi.rnu.tn

F. Ghorbel
e-mail: faouzi.ghorbel@ensi.rnu.tn

The graph-based approaches have the potential to code geometrical and topological shape properties in an intuitive manner. The usually used descriptors are Reeb graphs [14, 15] and the skeletal graphs [16].

For the fourth description category, numerical attributes (local or global) of the 3D object are collected. Several past works adopted this approach for invariant features extraction like the works of high curvature area determination [17, 18], the generalized shape distribution [19], the extend Gaussian image [20, 21], the 3D moments [22], and the canonical 3D Hough transform descriptor [23]. In order to verify as much as possible the wished criteria, authors in [24] have introduced a novel surface representation by iso-curvature features' computation. In [25], authors have proposed to generalize the SIFT algorithm, well known for 2D images, to 3D area. Other methods impose the use of local coordinates by the exponential map around a point belonging to the two-dimensional manifold obtained by wrapping a neighborhood of this point by the polar coordinates of the tangent plane at the same point or by constructing a set of geodesic circles relative to a given reference point [26–29]. Only the last category is invariant under the original parameterization. So the descriptors computed in the case of the three first methods depend largely on the choice of the mesh points. For this reason, we try in this work to improve the last category of description. The stability of the methods in [26–29] remains dependent on the robustness of the reference point detection.

In order to stabilize these last differential representations, we propose here a new representation that we call bipolar one. It consists on the construction of level sets of the superposition of the two geodesic potentials relative to a couple of reference points. An error made in the position of one of the two reference points will have fewer inferences on our proposed bipolar representation. Its robustness under the distortions of reference points positions will be studied.

Thus, this paper will be structured as follows: we describe in the second section the mathematical formulation of the proposed representation. In the third section, we present a comparison of two approximation methods. We illustrate in the fourth section the effectiveness of this representation for human face description. Subsequently, we evaluate in the sense of the shape distance its performance. We try to reach the exact value of this distance with an adapted version of the well-known Iterative Closest Point (ICP) algorithm introduced by Besl and Mckay in [30]. In the fifth section, we study its robustness under a given imprecision on positions of the reference points. We present in the sixth section a comparison between the proposed bipolar representation and some works from the state of the art.

2 Construction of the proposed invariant bipolar representation

Let us consider a two-dimensional differential manifold S and denote by U_r the scalar field of the geodesic potential generated from a reference point r. For each point p of S, $U_r(p)$ is the length of the geodesic curve joining p to r [31]. Such a function is well defined since a geodesic curve between any two points of the surface always exists. We note that for a given real value λ, a set of points forming a curve that we denote by C_r^λ is obtained. It belongs to the surface and is called the geodesic of level λ.

Let us consider now two reference points r and q of S and let denote by U_r and U_q their respective potential functions. It is easy to see that their corresponding gradients are orthogonal to the tangents of the related level curves. This fact comes from the retro-propagation equations [31]. Subsequently, we observe that along a geodesic, the tangent vectors to the level curves relative to the two potentials are parallel.

It is possible to prove that there always exist two levels λ^* and λ'^* such that the intersection between the two corresponding level curves extracted from r and q is not empty. Let us consider p^* an element of this intersection. Therefore, the angle formed by the two tangent vectors on p^* is zero when it belongs to the geodesic curve. It is easy to note that this angle increases continuously when p^* moves gradually away from this geodesic. The geometric locations having the same angular opening form a set of points of S. The points having the same angular opening are invariant. By considering a level set of angle, we construct a system of $SO(3)$-invariant points on S. These levels will be chosen so that they vary with the same constant from 0 to the integer K representing the maximum value determined by the interest region extend which lies between the two reference points and its neighborhood on the surface. Then, the descriptor can be written as following:

$$N_{r,q}^K(S) = \left\{ p^* \in S;\ |\langle T_{C_{\lambda^*,r}(t)}(p^*),\ T_{C_{\lambda'^*,q}(t')}(p^*)\rangle| = \alpha\frac{k}{K}, k = 0 \ldots K \right\} \quad (1)$$

where $T_{C_{\lambda^*,r}(t)}$ is the unit tangent vector to the level curve related to the reference point r on p^*, $<,>$ denotes the 3D inner product, and α is the maximum angular opening.

In summary, to construct the bipolar representation which corresponds numerically to the resolution of Eq. 1, the first step consists on the extraction of the two reference points from the surface. In the second step, the geodesic potentials generated from each reference point are computed. The relative level curves to these reference points are therefore computed with a constant geodesic step. A calculation phase of the intersection points between these level curves is established. Their corresponding tangent vectors are computed. Let us consider an intersection point between two such level curves. The angular opening formed by the two corresponding tangent vectors which can be considered as the inner product between these tangent vectors is computed. For a preselected levels set of these angular opening values, the corresponding intersection points are retained for the construction of the bipolar representation.

3 Discussion of the proposed representation approximations

The construction of the proposed representation supposes that the surface is a two-dimensional differential manifold. In this section, we compare two numerical methods for the implementation of the bipolar representation from the triangular mesh. The major difference between these two algorithms deals with the used approximation method of the tangent vectors.

Method 1 The first method consists on the tangent vector approximation by the differential of neighbor points of a discrete level curve. In practice, the description of a geodesic curve of level λ is extended to include a strip rather than a curve. It is composed by all mesh points with geodesic distances from a reference point that belong to $[\lambda-\epsilon, \lambda+\epsilon]$. ϵ is a positive real value which is suitably chosen according to the mesh resolution to avoid an intersection between two successive level curves.

Method 2 The second method is based on B-spline functions approximation [32] of the curve which can be written as follows:

$$C_k^{\lambda}(t) = \sum_{i=1}^{N_\lambda} B_{i,k-1}(t) \times \left(\left(1 - \frac{t-t_i}{t_{i+k}-t_i}\right) p_{i-1}^{r,\lambda} + \frac{t-t_i}{t_{i+k}-t_i} p_i^{r,\lambda}\right) \quad (2)$$

where $B_{i,k}(t)$ is the B-spline basic functions and $\{p_i^{r,\lambda}, i = 0...N_\lambda\}$ is the set of points that forms the geodesic discrete curve of level λ relatively to a given reference point r.

By deriving analytically this expression, the tangent vectors can be obtained for every t.

It is generally difficult to determine explicitly the expressions of geodesic curves on a real surface. However, for some mathematical surfaces such as cones, tori, cylinders, spheres, etc., it is possible sometimes to obtain their analytical expressions [33]. In order to illustrate and to verify the robustness of the two approximation methods, we propose to study the two geodesic potentials generated from two orthogonal poles on the unit sphere S^2. It is easy to see that the geodesic level curves relatively to each reference point are the parallel circles having the same central axis which is

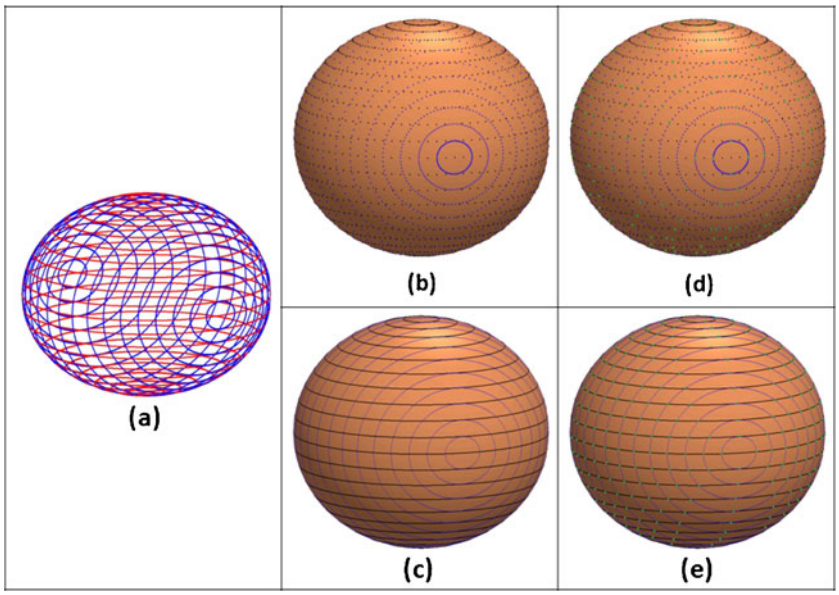

Fig. 1 **a** The geodesic level curves computed analytically. **b** The geodesic level curves extracted from the 3D mesh (method 1). **c** The geodesic level curves extracted from the 3D mesh (method 2). **d** The intersection points between the geodesic level curves (method 1). **e** The intersection points between the geodesic level curves (method 2)

the line passing through the pole and the sphere center. The discrete bipolar invariant set of points is constructed by the intersection points between these orthogonal circles. Figure 1 illustrates also the bipolar representation by the two different approximation methods.

These two approximation methods are applied to a sphere mesh and compared with the analytical one in the mean of the shape distance introduced by Ghorbel in [34, 35]. Following the same process, we denote by G the group representing all possible normalized parameterizations of surfaces which can be the real plane R^2 or the unit sphere S^2. We consider the space of all surface pieces as the set of all 3D objects assumed diffeomorphic to G which can be assimilated to a subspace of $L^2_{R^3}(G)$ formed by all square integrated maps from G to R^3. The direct product of the Euler rotations group $SO(3)$ by the group G acts on such space in the following sense:

$$SO(3) \times G \times L^2_{R^3}(G) \to L^2_{R^3}(G)$$
$$\{A, (u_0, v_0), S(u, v)\} \to AS(u + u_0, v + v_0) \quad (3)$$

The 3D Hausdorff shape distance Δ can be written for every S_1 and S_2 belonging to $L^2_{R^3}(G)$ and g_1 and g_2 to $SO(3)$ as follows:

$$\Delta(S_1, S_2) = \max(\rho(S_1, S_2), \rho(S_2, S_1)) \quad (4)$$

where

$$\rho(S_1, S_2) = \sup_{g_1 \in SO(3)} \inf_{g_2 \in SO(3)} \| g_1 S_1 - g_2 S_2 \|_{L^2} .$$

$\| S \|_{L^2}$ denotes the norm of the functional Banach space $L^2_{R^3}(G)$.

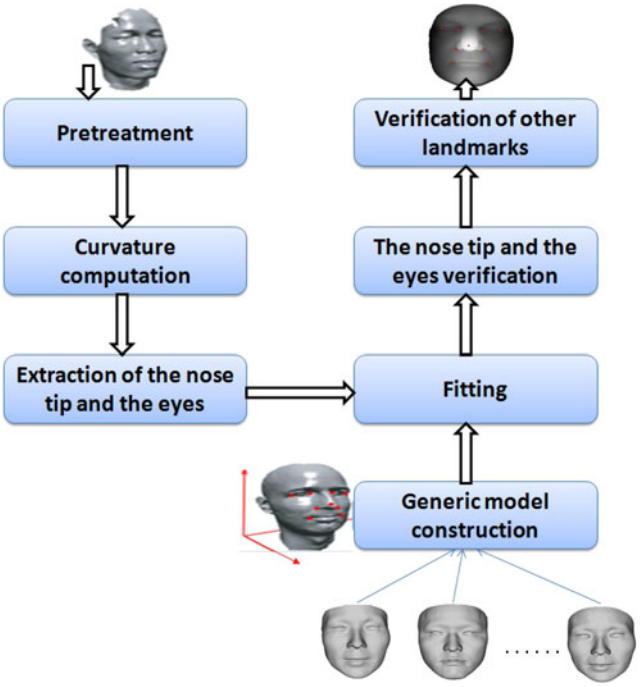

Fig. 3 The used algorithm for automatic reference points extraction

Due to the fact that the Euclidean rotations preserve this norm, it is easy to show that this distance is reduced to the following quantity:

$$\Delta(S_1, S_2) = \inf_{h \in SO(3)} \| S_1 - hS_2 \|_{L^2} . \quad (5)$$

After that, we consider a normalized version of Δ so that the variations of the normalized distance are confined to the interval [0, 1]. We propose to compute it for various level curve resolutions which are linked to the number of level curves relative to a geodesic potential generated from a reference point. The results are illustrated in Fig. 2.

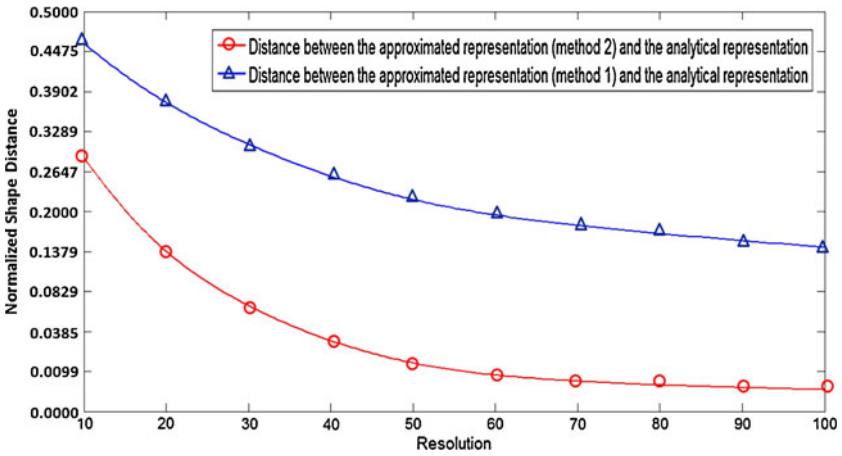

Fig. 2 The two normalized shape distances according to the resolution between the approximated representations and the analytical

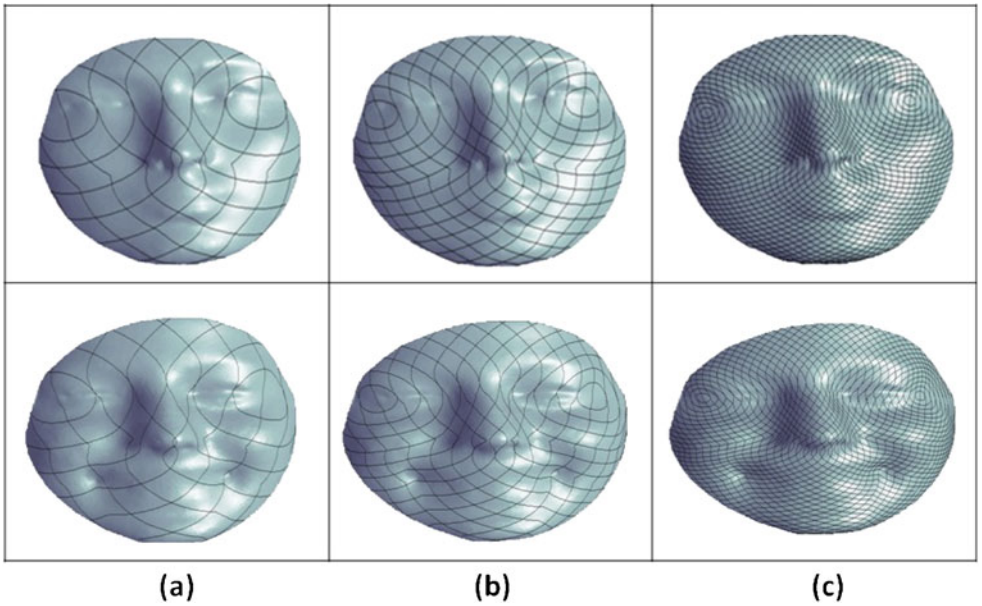

Fig. 4 *Row 1*: A neutral face. *Row 2*: A face with a happiness expression. **a** Five level curves between the two reference points. **b** Ten level curves between the two reference points. **c** Thirty level curves between the two reference points

With different resolutions, we can observe that the second method gives a better approximation of the proposed representation. The shape distance between the analytical representation and the one obtained by the second approximation method has a better behavior.

4 Description of human face surfaces

The three-dimensional face shape analysis has been an area of ongoing interest and research in image processing in the last two decades. It is attracting more and more attention with the development of 3D shape scanners and the availability of large 3D face databases [36]. We test, in this context, the accuracy of the bipolar representation on the 3D meshes of the database Bosphorus [37] using the second method of approximation. An evaluation in the sense of the shape distance is implemented to validate its performance. We use a total of ten faces that can be grouped into two classes. The first class contains five faces of the same person with different expressions and the second one contains five faces of different persons.

4.1 The choice of the two reference points

The first step of the bipolar representation construction consists on the choice of the two reference points from the face. It is important to select accurate reference points for shape representation. There is a general agreement that eyes are the most important facial features [38]. Indeed, they are a crucial source of information about the state of human being. Moreover, their appearance is less variant to certain face changes. Therefore, we choose to use the two outer corners of the eyes as reference points of the proposed bipolar representation.

4.2 Extraction of the two reference points

We refer here to the work of Szeptycki et al. [39] to extract automatically the two reference points which

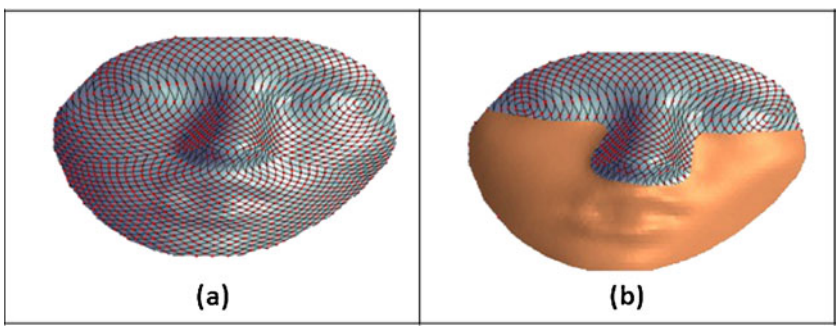

Fig. 5 **a** The invariant points in the whole face surface. **b** The invariant descriptor points only in the static area

are chosen to be the two outer corners of eyes. This method is based on a curvatures analysis with the use of a generic face model generated from a set of faces. Figure 3 summarizes this approach.

4.3 The computation of the geodesic distance

Having extracted the two reference points, we have to compute the geodesic distances between the two reference points and each vertex of the surface. Several past methods have been proposed to compute distances on discrete meshes. This computation must take in consideration the trade-off between the computational cost and the accuracy. We used in the present work a simple method in which the geodesic distance is approximated by Dijkstra's algorithm [40] based on the edges' length. This algorithm has a computational cost of order $O(n \log n)$. n is the number of vertices in the mesh.

4.4 Accuracy of the bipolar representation for human face description

After determining the two reference points and computing geodesic distances from these two points, the next step consists on the extraction of their corresponding level curves. Figure 4 illustrates the proposed representation for different resolutions.

Remark The completeness is an important property of a 3D representation. It gives ideas about the possibility to reach any point of the surface. For the proposed bipolar representation, this property can be observed. Indeed, from Fig. 4, we can note that, with more resolution, any point of the surface can be reached.

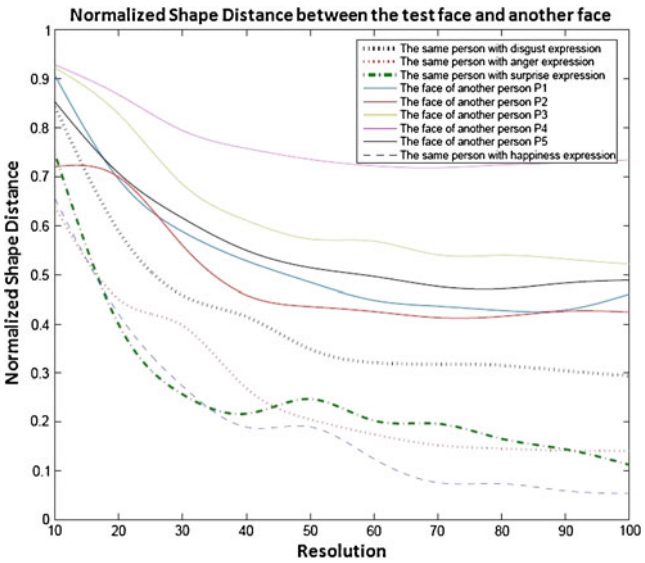

Fig. 6 Evolution of the normalized shape distance according to the resolution

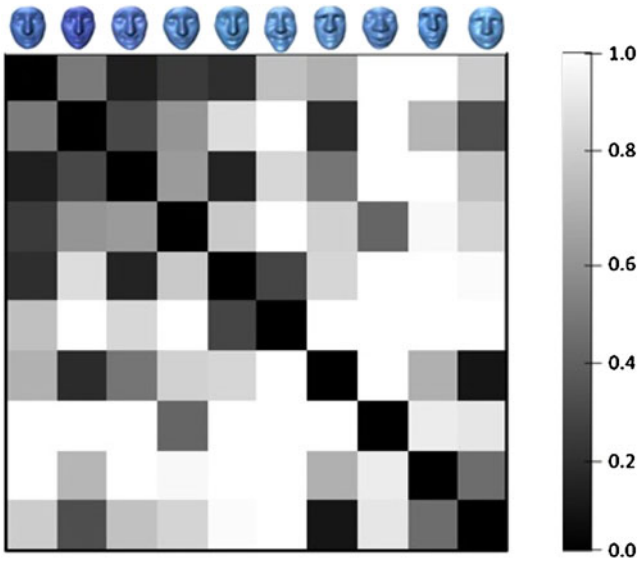

Fig. 7 Matrix of pairwise normalized shape distances between ten facial surfaces. The first five faces belong to the same person while the remaining are all different individuals

Different anatomical studies showed that the face can be divided into two areas: a static and mimic one. Thus, it is common to compute the descriptor only in the static area. Figure 5, which illustrates the geometric locations of the bipolar representation (a), shows also the invariant points of the static area obtained by a selection with a prior segmentation (b).

In order to evaluate the performance of this representation, the shape distance is implemented. The ICP algorithm tries to compute this distance between the representations of each of the two surfaces, with respect to a three-dimensional displacement, since its convergence is not guaranteed (local minima, etc.). Figure 6 shows different values of this distance according to the resolution. The neutral face of the first class is taken as test and others are expected to be the gallery faces. Figure 6 illustrates the coherence between the shape

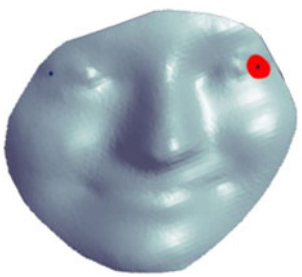

Fig. 8 The variation neighborhood of the outer corner of the left eye (with the *red color*)

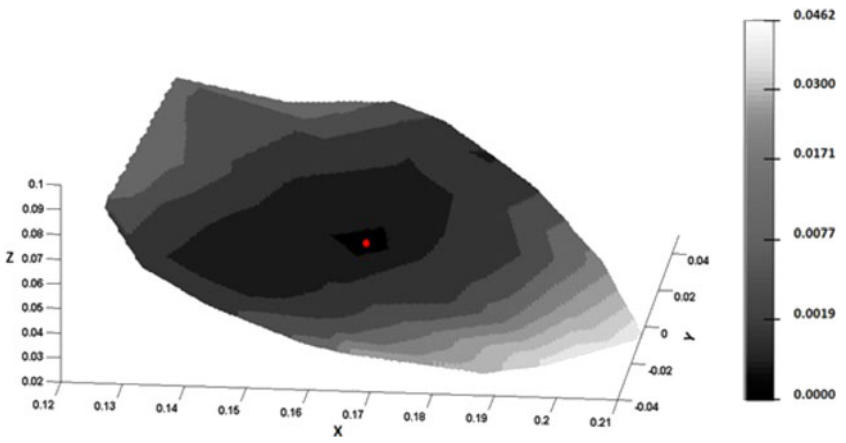

Fig. 9 The variation of the normalized shape distance according to the reference point localization

distance and the shape differences (between the test face and each face of the first class, between the test face and each face of the second class).

In order to illustrate the effectiveness of the joint introduction in this context of the two notions, the bipolar representation and the shape distance, the matrix representing the pairwise normalized distances between the ten faces is computed (see Fig. 7). The first five faces correspond to the first class. The rest belongs to the second class.

As expected, this matrix shows that the distances between the faces of the same person are smaller compared with the distances computed between faces of different persons.

5 Robustness under errors on reference points positions

In this section, we evaluate the robustness of the proposed bipolar representation under the variation of the reference points localization. Experimentations are performed on the three-dimensional faces of the database Bosphorus.

In order to evaluate experimentally the robustness of the proposed representation under the errors on the position of one of the two reference points, we assume that the outer corner of the left eye is moved by some geodesic distance around this point. This small position distortion does not exceed 5 % over the length of the geodesic curve joining the two outer corners of the eyes (see Fig. 8).

This evaluation is performed in the mean of the shape distance which is computed for the three following cases:

- The distance between the sampling points' set obtained from the bipolar representation without error on the positions of reference points (original representation) and the set generated by the same process applied to this representation with a given distortion on the outer corner of the left eye.
- The distances between the original set of invariant points and the same kind of invariant points extracted from the same face with different expressions.
- The distance between the original descriptors' set and points obtained with the same process coming from a face with another shape.

For the first case, the variations of this distance according to the reference point localization in this small neighborhood are illustrated in Fig. 9. The same

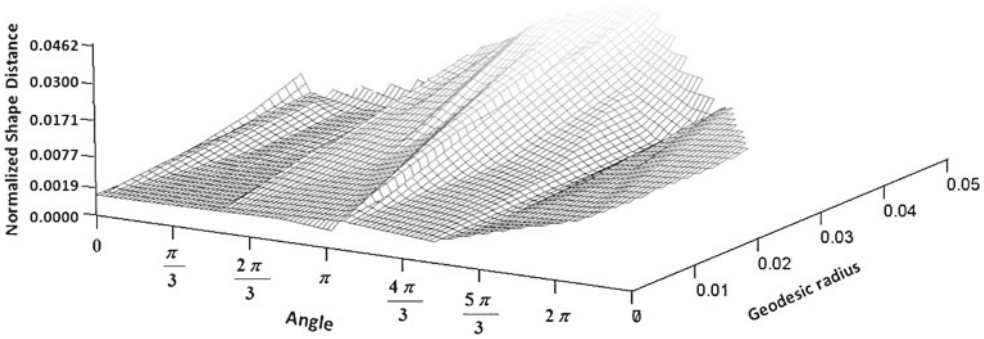

Fig. 10 The variation of the normalized shape distance according to the geodesic radius and the angle

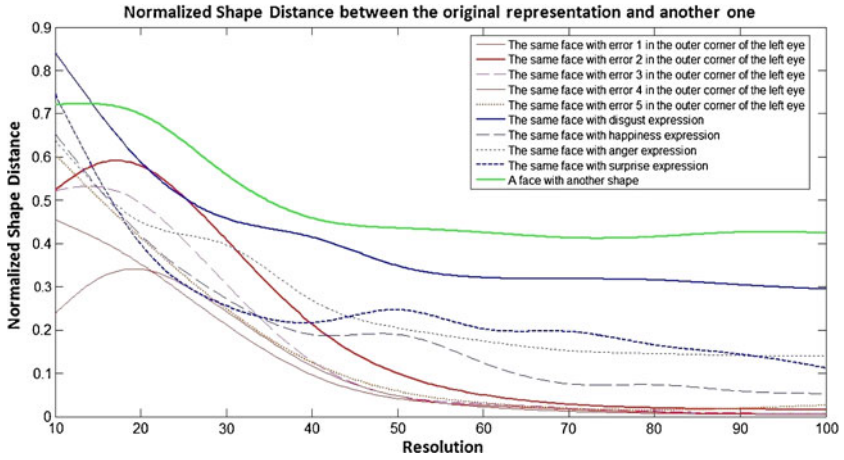

Fig. 11 Evolution of the shape distances according to the resolution for the three study cases

variation according to the geodesic radius and the angle is proven in Fig. 10. Figure 11 shows that the distance values obtained for the first case are relatively smaller than those obtained in the second case which are also smaller than the third one. Such results tend to prove the robustness of the proposed representation. Figure 11 indicates that there exists a convergence for a given resolution.

Several experimentations are performed in order to illustrate the robustness under distortions coming from natural variations of populations. For the first experimentation set, the second reference point (the outer corner of the left eye) is chosen randomly in a small neighborhood around the same point. The matrix representing the pairwise normalized shape distances between the ten faces is computed. Results are illustrated in Fig. 12.

For the second set of experimentations, the two reference points are fixed randomly in a small neighborhoods of the surface around the two original points. Results are illustrated in Fig. 13. We can note that, for the two experimentations series, the normalized distances between faces of the same person are smaller than the distances between different person faces.

These results show also the robustness of the bipolar representation under small variations of the reference points positions.

6 Comparison with some state-of-the-art methods

We compare in this section our bipolar representation with some works from the state of the art. We focus the comparison with the works of Bannour and Ghorbel [24], those of Samir et al. [27], and Srivastava et al.

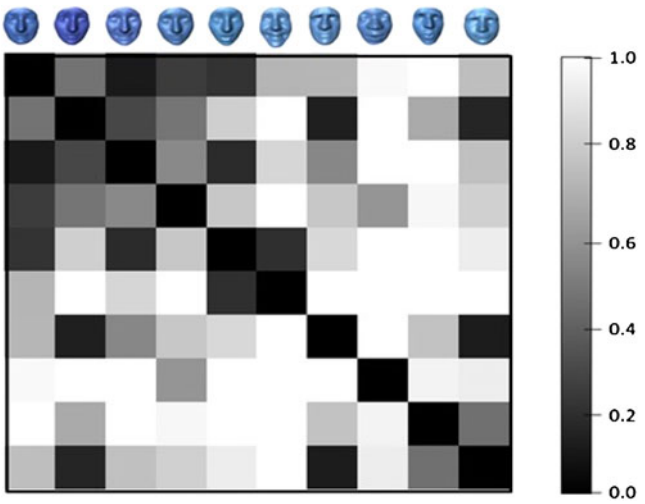

Fig. 12 Matrix of pairwise normalized shape distances between the ten faces with errors on the second reference point positions

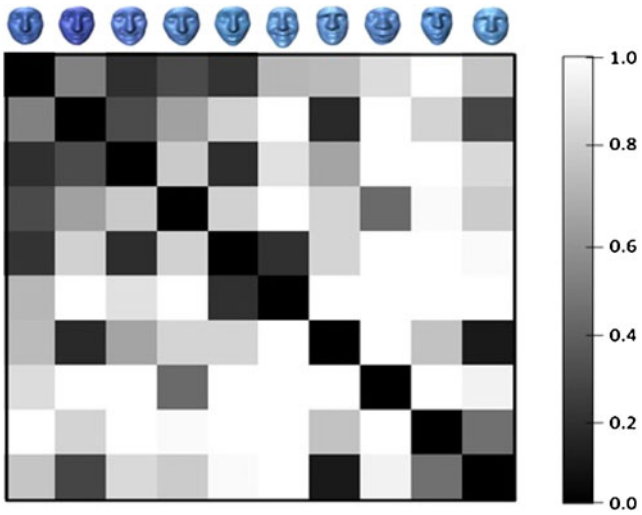

Fig. 13 Matrix of pairwise normalized shape distances between the ten faces with errors on the two reference points' positions

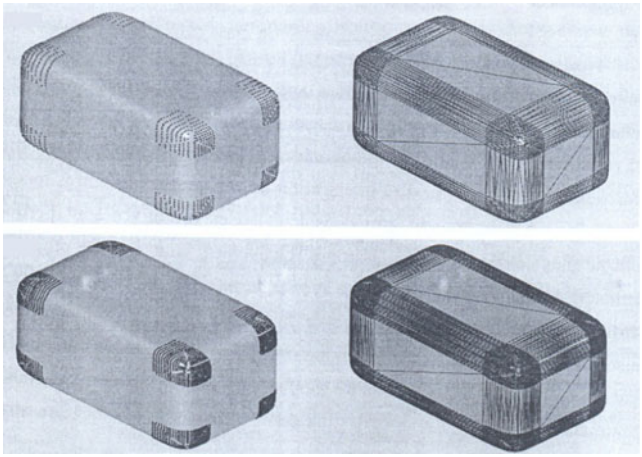

Fig. 14 An illustration of the representation of Bannour and Ghorbel obtained on a regular surface [24]

[28]. We study in the same sense the results obtained by Gadacha and Ghorbel [29].

6.1 Iso-curvature based representation

Bannour and Ghorbel have proposed a surface pseudo reparametrization [24]. It is based on the extraction of an invariant curves network. These curves are obtained by considering the levels' set of the principal curvature field of a given regular surface. This representation gives a solution to the visualization of enormous size surfaces. The weakness of such representation consists on the successive derivatives which are needed for the computation of the curvatures. This fact induces numerical errors on the curves' geometrical localization. Figure 14 illustrates the obtained representation.

Fig. 16 An illustration of the representation of the work of Gadacha and Ghorbel

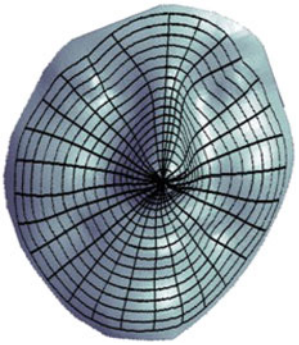

6.2 The levels set of facial curves

The efficiency of the two methods proposed by Samir et al. [27] and Srivastava et al. [28] has been observed in the face recognition field. However, these approaches can be criticized on two main points:

- An important complexity: The matching surfaces step is subdivided into two subproblems. In fact, each face surface is composed by a collection of indexed level curves constructed around the nose tip which is chosen to be the reference point. In order to compute the proposed distance between two faces, the first step consists on matching between corresponding level curves. After that, a procedure of matching points between corresponding level curves is implemented. This fact increases the computational complexity of the proposed algorithm.
- There is a discrimination between the information that operates on consecutive level curves. Indeed, these approaches suppose that each level curve is a main object that undergoes several transformations without taking into account the other level curves. We present in Fig. 15 an example that shows the

Fig. 15 An illustration of the two surfaces S and S_1

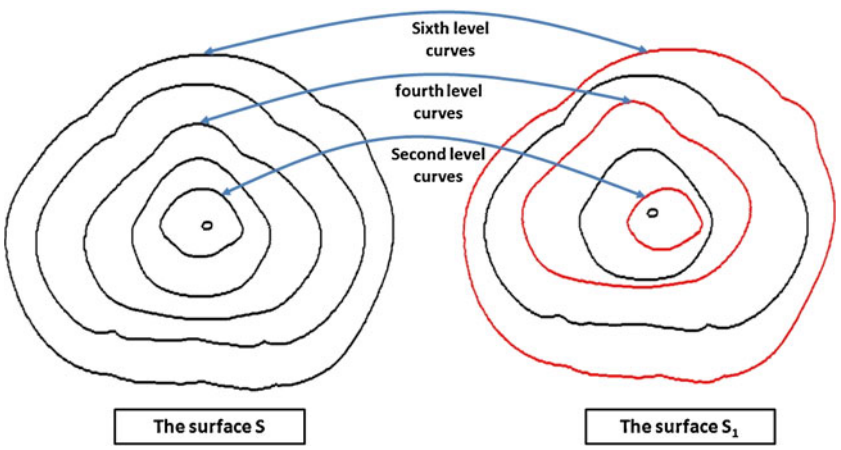

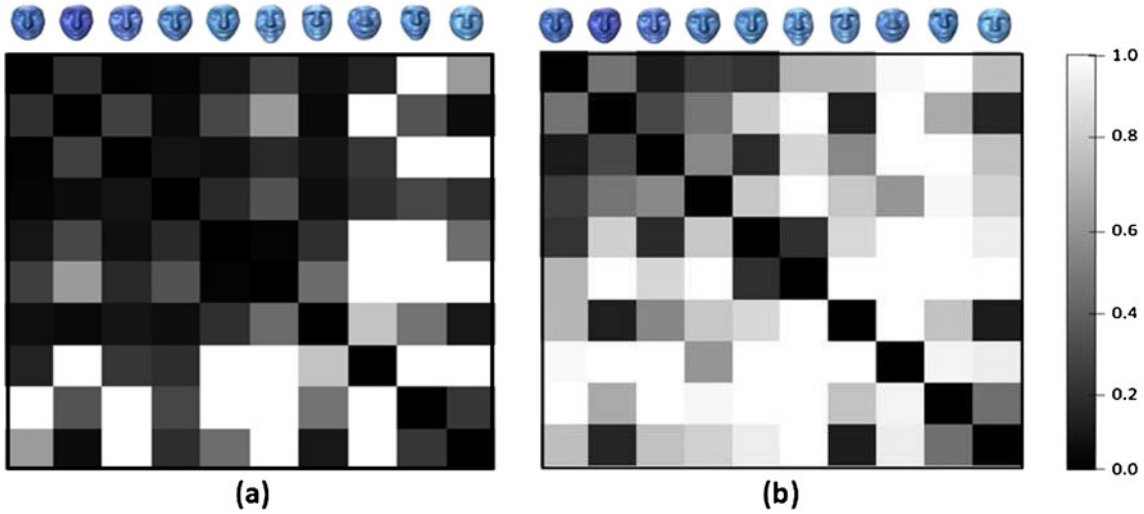

Fig. 17 **a** Matrix of pairwise normalized shape distances between the ten faces with errors on the nose tip point positions (the work of Gadacha and Ghorbel). **b** Matrix of pairwise normalized shape distances between the ten faces with errors on the outer corner of the left eye point positions (the proposed bipolar representation)

consequences of this fact. Let us consider a facial surface S composed of six indexed level curves. We apply random rotations respectively on the second level curve, the fourth level curve, and the sixth level curve so that we obtain a new surface S_1 as illustrated in Fig. 15. In these works, the proposed distance between two matched level curves is invariant under different reparametrizations and rotations. Then, the summation of any matched level curves' distances is near to zero; however, the global shape of the two surfaces seems to be very different.

6.3 The levels set of Darcyan coordinates

The sampling of the well-known Darcyan coordinates system computed around a given point of the surface gives a set of organized invariant points. In [29], authors propose to find an optimal sampling parameter which is fixed with the application of a generalization version of Shannon theorem to a surface parametrization. Such representation is generally used around all critical points on a studied surface. Figure 16 illustrates this representation.

In the same paper, it has been shown that such representation is useful for fast registration procedures. However, this method suffers from the position of the reference point. We propose to make a comparison between this representation and our bipolar one in the sense of the robustness under errors on the reference points' extraction. The shape distance is used as a metric of comparison. We move the nose tip in the representation of Gadacha and Ghorbel and the outer corner of the left eye used in the bipolar representation by the same geodesic distance around the original points (with good extraction). The matrices representing the pairwise normalized shape distances between the ten faces are computed for the two cases. Results are illustrated in Fig. 17. From the observation of the two matrices, we can note that the bipolar representation ensures more robustness under errors on the extraction of the reference points.

7 Conclusion

In this paper, we have introduced a novel invariant surface representation under 3D rigid transformations. It is based on the superposition of the two geodesic potentials generated from the two reference points. It is an attempt to generalize what is known by local coordinates around a reference point. This new representation tries to stabilize these coordinate systems which are dependent on the reference point detection. Two numerical methods have been studied. In order to retain the efficient approximation algorithm, these methods have been compared. The robustness of our representation under small variations in reference points' positions has been analyzed. Experimentations performed on the 3D faces databases have identified the discrimination power of such representation in the sense of the normalized Hausdorff shape distance. A comparison of the proposed bipolar representation

with some works from the state of the art has been established.

The perspectives of this work will involve the implementation of this description for other types of applications (medical, archeological, etc.). We propose, in the future works, to order the constructed invariant points from the proposed representation. We intend also to extend it to a number of reference points greater than two and to develop a theoretical analysis of its locality extend limits.

References

1. Dutagaci H, Sankur B, Yemez Y (2005) Transform-based methods for indexing and retrieval of 3D objects. In: Fifth international conference 3D digital imaging and modeling, pp 188–195
2. Burdin V, Ghorbel F, Tocnaye JDBDL, Roux C (1992) A three-dimensional primitive extraction of long bones obtained from bi-dimensional Fourier descriptors. Pattern Recogn Lett 13(3):213–217
3. Daras P, Zarpalas D, Tzovaras D, Strintzis MG (2004) Shape matching using the 3D Radon transform. In: Second international symposium 3D data processing, visualization, and transmission, pp 953–960
4. Zarpalas D, Daras P, Axenopoulos A, Tzovaras D, Strintzis MG (2007) 3D model search and retrieval using the spherical trace transform. EURASIP J Adv Signal Process 2007(1):14
5. Ricard J, Coeurjolly D, Baskurt A (2005) Generalizations of angular radial transform for 2D and 3D shape retrieval. Pattern Recogn Lett 26(14):2174–2186
6. Vranic DV (2003) An improvement of rotation invariant 3D shape descriptor based on functions on concentric spheres. In: IEEE international conference on image processing, pp 757–760
7. Kazhdan M, Funkhouser T, Rusinkiewicz S (2003) Rotation invariant spherical harmonic representation of 3D shape descriptors. In: Eurographics/ACM SIGGRAPH symposium on geometry processing, pp 156–164
8. Bel Hadj Khelifa W, Ben Abdallah A, Ghorbel F (2008) Three dimensional modeling of the left ventricle of the heart using spherical harmonic analysis. In: 5th IEEE international symposium on biomedical imaging: from nano to macro (ISBI 2008), Paris, France
9. Brechbuhler C, Gerig G, Kubler O (1996) Parametrization of closed surfaces for 3-D shape description. Comput Vis Image Underst 16:154–170
10. Papadakis SPP, Pratikakis I, Theoharis T (2007) Efficient 3D shape matching and retrieval using a concrete radialized spherical projection representation. Pattern Recogn 40(9):2437–2452
11. Laga H, Takahashi H, Nakajima M (2006) Spherical wavelet descriptors for content-based 3D model retrieval. In: IEEE international conference on shape modeling and applications, pp 15–25
12. Chen DY, Tian XP, Shen YT, Ouhyoung M (2003) On visual similarity based 3D model retrieval. Computer Graphics Forum 22(3):223–232
13. Vranic DV (2004) 3D model retrieval. PhD dissertation, University of Leipzig
14. Hilaga M, Shinagawa Y, Kohmura T, Kunii TL (2001) Topology matching for fully automatic similarity estimation of 3D shapes. In: ACM SIGGRAPH, pp 203–212
15. Tung T, Schmitt F (2005) The augmented multiresolution Reeb graph approach for content-based retrieval of 3D shapes. Int J Shape Model 11(1):91–120
16. Sundar H, Silver D, Gagvani N, Dickinson S (2003) Based shape matching and retrieval. In: Shape modeling international 2003, p 130
17. Faugeras OD, Hebert M (1986) The representation, recognition and positioning of 3D shapes from range data. In: Rosenfeld A Techniques for 3D machine perception. North-Holland, Amsterdam
18. Hallinan PW, Gordon GG, Yuille AL, Giblin P, Munford D (1999) Two and three dimensional patterns of face. A.K. Peters, Wellesley
19. Liu Y, Zha H, Qin H (2006) The generalized shape distributions for shape matching and analysis. In: IEEE international conference of shape modeling and applications, p 16
20. Horn BKP (1984) Extended Gaussian images. Proc IEEE 72(12):1671–1686
21. Kang SB, Ikeuchi K (1993) The complex EGI: a new representation for 3D pose determination. IEEE Trans Pattern Anal Mach Intell 15(7):707–721
22. Sadjadi FA, Hall EL (1980) Three-dimensional moment invariants. IEEE Trans Pattern Anal Mach Intell 2(2):127–136
23. Zaharia Z, Preteux F (2002) Shape-based retrieval of 3D mesh models. In: IEEE international conference on multimedia and expo (ICME 2002), Lausanne, Switzerland
24. Bannour MT, Ghorbel F (2000) Isotropie de la représentation des surfaces; Application à la description et la visualisation d'objets 3D. In: RFIA 2000, pp 275–282
25. Scovanner P, Ali S, Shah M (2007) A 3-dimensional sift descriptor and its application to action recognition. In: 15th international conference on multimedia
26. Spivak M (1999) A comprehensive introduction to differential geometry. Publish or Perish, Houston
27. Samir C, Srivastava A, Daoudi M (2006) Three dimensional face recognition using shapes of facial curves. IEEE Trans Pattern Anal Mach Intell 28(11):1858–1863
28. Srivastava A, Samir C, Joshi SH, Daoudi M (2008) Elastic shape models for face anlysis using curvilinear coordinates. J Math Imag Vis 33(2):253–265
29. Gadacha W, Ghorbel F (2012) A new 3D surface registration approach depending on a suited resolution: application to 3D faces. In: IEEE Mediterranean and electrotechnical conference (MELECON), Hammamet, Tunisia
30. Besl PJ, Mckay ND (1992) A method for registration of 3-D shapes. IEEE Trans Pattern Anal Mach Intell 14(2):239–256
31. Cohen LD, Kimmel R (1997) Global minimum for active contour model: a minimal path approach. Int J Comput Vis 24(1):57–78
32. Demengel G, Pouget JP (1998) Mathématiques des courbes et des surfaces: modeles de Bezier, des B-splines et des nurbs. Edition Ellipses
33. Struik DJ (1988) Lectures on classical differential geometry. Dover, New York
34. Ghorbel F (1998) A unitary formulation for invariant image description: application to image coding. Ann Telecommun (Special issue) 53(5–6):242–260
35. Ghorbel F (2012) Invariants for shapes and movement. Eleven cases from 1D to 4D and from Euclidean to projectives (French version). Arts-pi Edition, Tunisia
36. Phillips PJ, Flynn PJ, Scruggs T, Bowyer KW, Chang J, Hoffman K, Marques J, Min J, Worek W (2007) Overview of the face recognition grand challenge. In: IEEE conference

on computer vision and pattern recognition workshops, pp 947–954
37. Savran A, Alyz A, Dibeklioglu H, Eliktutan O, Gkberk B, Sankur B, Akarun L (2008) Bosphorus database for 3D face analysis. In: The first COST 2101 workshop on biometrics and identity management (BIOID2008)
38. Campadelli P, Lanzarotti R, Lipori G (2007) Automatic facial feature extraction for face recognition. In: Delac K, Grgic M (eds) Face recognition. I-Tech Education and Publishing, Vienna. ISBN: 978-3-902613-03-5
39. Szeptycki P, Ardabilian M, Chen L (2009) A coarse-to-fine curvature analysis-based rotation invariant 3D face landmarking. In: IEEE 3rd international conference on biometrics: theory, applications, and systems, 2009. BTAS '09
40. Dijkstra EW (1959) A note on two problems in connection with graphs. Numer Math 1:269–271